Available online at www.sciencedirect.com
SCIENCE DIRECT®
Journal of Photochemistry and Photobiology A: Chemistry 165 (2004) 241–246
Journal of Photochemistry and Photobiology A:Chemistry
www.elsevier.com/locate/jphotochem

Titanium dioxide sol–gel deposited over glass and its application as a photocatalyst for water decontamination

Silvia Gelover [a,*], Pedro Mondragón [b], Antonio Jiménez [b]

[a] *Instituto Mexicano de Tecnología del Agua, IMTA, Paseo Cuauhnahuac 8532, Progreso, Jiutepec, Morelos 62550, Mexico*
[b] *Centro de Investigación en Energía, CIE-UNAM Priv. Xochicalco s/n. Col. Centro. Temixco, Morelos 62580, Mexico*

Received 22 August 2003; received in revised form 17 March 2004; accepted 25 March 2004

Abstract

Photocatalytic degradation of water pollutants using TiO_2 and solar light has been proposed as an effective alternative of treatment. Usually, TiO_2 as a finely divided powder is added to polluted water forming a suspension, which is then irradiated under sunlight to conduct photochemical reactions. Although the literature frequently points out the minor efficiency of immobilized systems, it is desirable to look for a fixed catalyst to avoid wastes of time and materials during separation of the powder at the end of the treatment. This paper presents results that show the use of anatase thin films as an efficient form of deposited TiO_2 for the photocatalytic degradation of 4-chlorophenol, a priority pollutant commonly used as a model in photocatalysis, and for carbaryl, a carbamic pesticide. The thin films were deposited over small cylindrical pieces of glass, using a sol–gel technique, the average thickness being 600 nm, and having a band gap of 3.28 eV. The anatase TiO_2-covered glasses were used to fill a cylindrical photoreactor located at the focus of a parabolic solar collector able to concentrate up to 41 suns. Results show that the films are an effective catalyst in photodegradation, under solar irradiation, and conduct to similar values as those for TiO_2 in suspension. The photoefficiency obtained is similar to that obtained using powder suspension. These results compel us to the continued pursuit of TiO_2 immobilization.
© 2004 Elsevier B.V. All rights reserved.

Keywords: Titanium dioxide films; Solar photocatalysis; TiO_2 immobilization

1. Introduction

During the last decades several efforts have been focused on improving decontamination of air and water [1]. One of the most attractive options is the treatment by oxidation using a semiconductor, typically titanium dioxide, in combination with solar radiation. This process can destroy organic matter, transforming organic carbon to CO_2 and organic N, S or Cl to diluted inorganic acids (HNO_3, H_2SO_4 and HCl), employing just solar energy and a low cost non-toxic catalyst.

This kind of treatment is presently found at the level of pilot treatment plants. The system uses TiO_2 in slurry photoreactors, which is recovered after the treatment [2,3]. An immobilized form of the catalyst is beneficial since it requires less time, reduces losses of materials and skips recuperation steps of the catalyst. Immobilization of TiO_2 has been largely wanted as it is shown in the review by Pozzo [4] and in more recent publications [5–7]. The published results are not enough to clearly establish the benefits of supported TiO_2 against its suspended form.

In this paper, we present results for solar detoxification of water using films of TiO_2 supported over small glass cylinders. The tested pollutants were carbaryl (CB) and 4-chlorophenol (4-CP). Carbaryl is a carbamic pesticide of intensive application in Mexico, and 4-CP is an organochloride compound used as a model in photocatalysis [8–12]. The fixed form of TiO_2 presented is as effective as the Degussa P-25 powder, which is recognized as the most efficient form of titanium dioxide. Considering the great operational advantages of the supported catalyst, this is a promising idea that must be considered for future design of effective photocatalytic processes.

2. Experimental

2.1. Preparation of the films

For the preparation of the films, a sol–gel system was obtained based on a published recipe [13] where 0.1 mol of titanium isopropoxide (Ti(i-$C_3H_7O_2$)$_4$, Aldrich, 97% purity)

* Corresponding author. Tel.: +52-7773293664; fax: +52-7773293664.
E-mail addresses: sgelover@tlaloc.imta.mx (S. Gelover), ajg@mazatl.cie.unam.mx (A. Jiménez).

1010-6030/$ – see front matter © 2004 Elsevier B.V. All rights reserved.
doi:10.1016/j.jphotochem.2004.03.023

was mixed with 0.4 mol of ethanol (absolute grade, Monterrey), both used as-received. Titanium isopropoxide was hydrolyzed by slow addition of a cold (4 °C) mixture consisting of 0.1 mol of deionized water and 0.008 mol of hydrochloric acid diluted in 0.4 mol of ethanol. The acid is added to catalyze the hydrolysis. The final mixture was maintained under magnetic agitation at least 8 h at room temperature. If the mixture is kept tightly closed, it remains stable for at least 45 days.

The films employed were deposited in small cylinders of Pyrex glass (6 mm external diameter, 4 mm internal diameter and 6 mm long). To obtain the films, an immersion system with a withdrawal speed of 10 cm min^{-1} was employed. Three successive immersion cycles (sol–gel deposition plus heat treatment) of the substrates were carried out in the sol mixture described in the previous paragraph. After each immersion, the films were annealed in air at 500 °C. In order to treat the adsorbed films thermally, the glass cylinders were put over aluminum supports, introduced into a furnace set at the given temperature for 10 min. For the optoelectronic characterization, the film deposition was also carried out over rectangular microscope slides (25 mm × 70 mm × 1 mm) of Pyrex glass using the same immersion system at the same controlled withdrawal speed.

2.2. Films characterization

Grain size as well as crystalline phase of TiO_2 films was determined using an X-ray Diffractometer (DMAX/2000), Rigaku. Making a scratch on the film, its thickness was measured in an alpha-step 100 profilometer from Tencor Instruments. The band gap was calculated using optical transmittance and specular reflectance spectra measured in a spectrophotometer Shimadzu 1100 UV-Vis-near IR. An electrometer/multimeter Keithley 619 was used for photoresponse measurements employing a halogen/tungsten 100 W lamp. Two silver electrodes (1 cm long parallel lines, separated 1 cm) were painted over the films and a 10 V voltage was applied between them. The electrical current is measured as a function of time for a dark–light–dark step, to obtain σ_{light} and σ_{dark} values and then photosensitivity $S(= (\sigma_{light} - \sigma_{dark})/\sigma_{dark})$.

2.3. Photoreactor

The experimental device used in the treatment of polluted water has been described elsewhere [14]. It is basically a circulating system conducting water through a parabolic trough collector concentrating 41 times the solar radiation. In the focus of the collector there is a Pyrex glass tube (2.5 cm internal diameter, 1.7 m length), containing the small covered TiO_2 cylinders. For comparison purposes slurries of the same spiked water containing TiO_2 powder, at 1 g/l (Degussa), were irradiated in the same collector.

2.4. Reactives

All the chemicals employed here were reactive grade, except when indicated. In the case of ethanol its initial grade was absolute and it was not distilled prior to use. The TiO_2 powders employed in this job were from Aldrich (99% anatase) and Degussa (70% anatase:30% rutile). For carbaryl degradation experiments, an agricultural formulation containing 80% of active ingredient (carbaryl) was employed, and for 4-chlorophenol, a pure reactive standard.

2.5. Analytical measurements

Carbaryl concentration variations during photodegradation processes were followed by the changes in the absorbance spectra of the reaction mixture in the UV region. Aliquots absorbance was determined in a HP-8542 diode array spectrophotometer ($\lambda = 288$ nm). In some selected experiments, the carbaryl concentration was measured by HPLC. In the case of the 4-chlorophenol (4-CP), the concentration variations were monitored using a HPLC-UV detector (column C18, mobile phase acetonitrile:water 30:70, $\lambda = 280$ nm).

2.6. Degradation experiments

In each case, samples of 1.5 L of water spiked with the pollutant (20 mg/L) were circulated in the experimental device for 3 h under solar radiation (average direct radiation 645 W/m^2). In order to reach adsorption plateau the samples were circulated 5 min before irradiation. Aliquots of 5 mL were withdrawn at selected times for analysis. Samples containing TiO_2 powder, at 1 g/L, were filtered through 13 mm HPLC syringe filters of 0.2 μm nylon, immediately after sampling.

Additional tests were performed to improve photooxidation through the use of hydrogen peroxide as an additional source of $OH^{\bullet}$ radicals. In the case of carbaryl, hydrogen peroxide was added (3 g/L) before irradiation. For 4-chlorophenol, 2 mL of commercial grade (50%) hydrogen peroxide were added after each aliquot withdrawn for the target pollutant determination, at sampling times: 0, 15, 30, 60, 90 and 120 min. In order to avoid overestimation, due to the presence of the peroxide, it was necessary to prepare a specific blank for each measurement during spectrophotometric quantification of 4-CP.

2.7. Toxicity

In the case of 4-chlorophenol, measurements of toxicity in the initial and final samples were obtained. Toxicity was measured with Vibrio fischeri as the test organism. The effective concentration toxicant estimated to cause a 50% decrease in the luminosity of test organisms, EC_{50}, was measured [15].

3. Results

3.1. Crystalline structure of TiO_2 films

The XRD characterization of the TiO_2 films revealed anatase as the predominant crystalline phase (Fig. 1). According to JCPDS 21-1272, anatase presents the following diffraction pattern: A major intensity signal associated to the reflection (1 0 1) located at $2\theta = 25.28^\circ$ (relative intensity 100%), as well as other important signals at 37.8° (20%), 48.05° (35%), 53.89° (20%), 55.06° (20%), and 62.69° (14%) and θ is the Bragg's angle of the diffraction peak. All these signals were present in our films.

The grain size has been calculated from the XRD patterns using the Scherrer's equation: $D = 0.9\lambda/\beta\cos\theta$ [16], where λ is the wavelength of the X-ray, β the full width (radians) at half maximum (FWHM) of the signal. The calculated values were similar to those obtained with the integrating software Jade 5.0, from Materials Data Inc. (MDI). A crystallite size of 13–16 nm was calculated. No attempt was made to arrive at a more exact estimation of the particle size.

An average film thickness of 598 nm (three sol–gel immersion cycles) was selected as adequate for the immobilized catalysts. Film thickness was used to calculate the quantity of immobilized TiO_2 over the glass rings, assuming a density value of 3.41 g cm^{-3} for anatase [17]. From this, a relation of 1.2 g of TiO_2 per liter of treated sample could be estimated, which is similar to the 1 g/L used for the powder slurry.

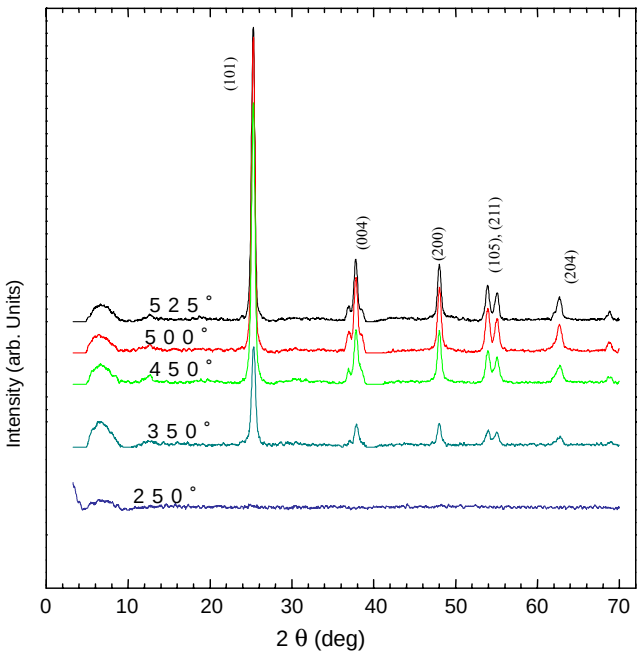

Fig. 1. X-ray diffraction patterns of TiO_2 films ($d = 1984$ nm) deposited by the sol–gel technique and treated at different annealing temperatures.

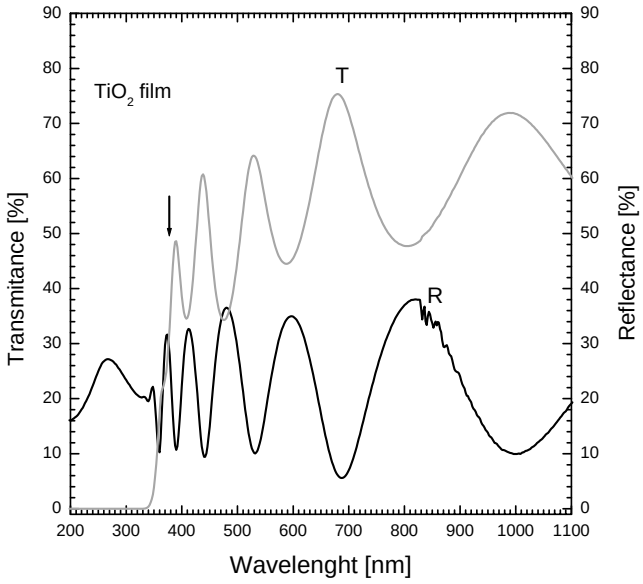

Fig. 2. Optical transmittance and reflectance spectra for a TiO_2 film with a thickness of 598 nm.

3.2. Optical properties

Fig. 2 shows the optical transmittance (T, %) and the reflectance (R, %) spectra of representative samples of the TiO_2 films. The observed modulations in the transmittance as well as in the reflectance spectra are indicative for a well formed film on the glass substrate. Focusing attention on the transmittance spectrum, the optical transmittance begins to decrease drastically at a wavelength of about 380 nm (3.26 eV), as indicated by the arrow above the transmittance curve. This fact indicates that the optical absorption in TiO_2 starts at that wavelength. Therefore, a value of 380 nm approaches to the crucial wavelength for the optical absorption.

Using optical transmittance and reflectance spectra from Fig. 2, it was possible to determine the absorption coefficient and band gap of TiO_2 films. Considering that the diffuse reflectance is negligible, the expression for the absorption coefficient α is $(1/d) \times \ln[100 - R_{sp}/T]$, where d is the film thickness, R_{sp} the optical reflectance and T the transmittance. The optical band gap for allowed indirect transitions can be evaluated from a $\alpha^{1/2}(h\nu)^{1/2}$ versus $h\nu$ plot, where $h\nu$ is the energy of the incident radiation [18,19]. TiO_2 thin films have an indirect band gap of 3.28 eV, which is very close to the band gap value reported by other researchers [20].

This band gap value is in agreement with the estimated value from the transmittance spectrum (3.26 eV) shown in Fig. 2. Also, TiO_2 thin films show a direct band gap of 3.56 eV for allowed transitions, which has been calculated from a $\alpha^2(h\nu)^2$ versus $h\nu$ plot [18,19].

3.3. Electrical properties

Having the catalyst in the form of a film offers a variety of advantages. From a practical point of view, it saves time

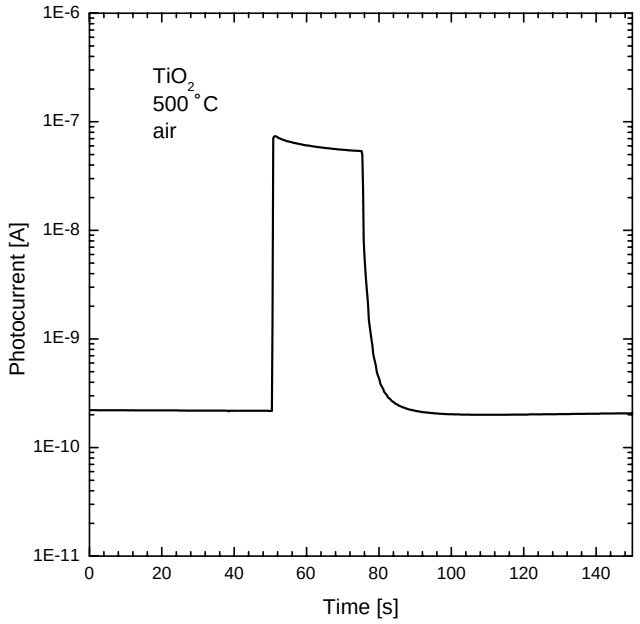

Fig. 3. Photoresponse curve of a TiO_2 film with a thickness $d = 598$ nm.

before analysis of processed samples as well as at the end of treatment as it does not require separation of the catalyst. On the other hand, some properties such as electrical conductivity and photosensitivity can be measured easily in the films while similar estimations are hardly conducted in powder catalysts.

The photosensitivity, an important property as it is closely related to the capability of the material to generate electron–hole pairs under UV radiation, is directly estimated from electrical conductivity measurements. Fig. 3 shows the photoresponse (photocurrent) curve of sol–gel prepared TiO_2 film with a thickness d of 598 nm.

A dark current from 2.2×10^{-10} A is observed giving an electrical dark conductivity of $1.45 \times 10^{-7}\,[\Omega\,\mathrm{cm}]^{-1}$. An explanation for the dark conductivity lies on the n-type semiconductor character of TiO_2. It is well known that TiO_2 is a n-type semiconductor. When the thickness increases, the TiO_2 films achieve bulk properties, as found in macro-size particles. It is also well known that the n-type character of metal oxides is given by an oxygen deficiency and that oxygen vacancies act as electron donors, which is favored by the thermal treatments [21,22]. Therefore, the dark current of the TiO_2 achieves bulk values when the film thickness increases.

Under illumination, the electrical current grows sharply due to the absorption of photons with energy equal or greater than band gap value, which increases the electron concentration in the conduction band. The photoresponse grows up as thickness does, up to a specific thickness d_o. Over d_o, dark and light current start to decrease because the surface is not as homogeneous. For thicknesses bigger than 2000 nm, films begin to crack and peel off. Related to the dark current value, we observe a current increase near to two magnitude orders and a photoconductivity σ_{light} of $1.31 \times 10^{-4}\,[\Omega\,\mathrm{cm}]^{-1}$. Considering a TiO_2 thin film of 598 nm thick, its calculated photosensitivity value $S(= (\sigma_{light} - \sigma_{dark})/\sigma_{dark})$ is 2.91×10^2. This is a high photosensitivity value compared to the powder photosensitivity for commercial TiO_2 catalysts ($<10^1$). Therefore, photoexcited electrons in the conduction band are responsible for the achieved high current values under the applied external field.

Once the light is turned off, the electron–hole recombination takes place; electrons fall down into the valence band under emission of photons (fluorescence) or Auger electrons, as predominant relaxation processes. Due to the very sharp increase and decrease of the photocurrent by turning on and off light, respectively, we can affirm that the existence of energy levels (like trapping levels) inside the band gap is not a continuous distribution and is negligible, suggesting that TiO_2 is a highly pure material. The good quality film is confirmed by the interference pattern observed in the UV-Vis transmittance and reflectance spectra (Fig. 2).

Taking into account the existent compromise between film thickness and optical transmittance, to get simultaneously a high photosensitivity and a high transmittance, a film thickness of 598 nm was selected as optimal (2.91×10^2 photosensitivity and ~70% transmittance). So, this film thickness was used for the sol–gel deposition of TiO_2 films over glass cylinders considering that in the photoreactor, the light must pass through the cylinder walls. Depending on the final requirements and uses, it is possible to get thicker TiO_2 films (up to a determined thickness d_o), which gives the possibility to obtain higher photodegradation rates, as has been found by other authors [7]. The TiO_2 thin films are proposed here as an alternative to slurries used in photocatalytic degradation processes. Therefore, an important task to be done is to compare the capability of TiO_2 thin films against powder form to photodegrade target pollutants.

3.4. Solar photocatalytic degradation of carbaryl

Fig. 4 shows photodegradation curves for carbaryl using (a) Degussa P-25 and (b) TiO_2 thin films as catalysts. Curve (c) is the same as (b) but adding H_2O_2 as oxidant agent. Using the powder form of the catalyst, after 180 min of irradiation, the carbaryl concentration (measured as absorption at 288 nm) reached final values around 41.1% of the initial pesticide concentration.

The carbaryl concentration measured by HPLC (not shown in Fig. 4) was always smaller than the value determined by the spectrophotometer UV-Vis. After the photocatalytic treatment, the HPLC final carbaryl concentration was around 34.7% of the initial value. It is clear that UV measurements are not exclusively due to carbaryl but also to other UV absorbers present in the reaction mixture, such as naphtol and naphtoquinones described as phototransformation products in aqueous solution [23]. It is not the aim of this work to have a deep insight of the photocatalysis

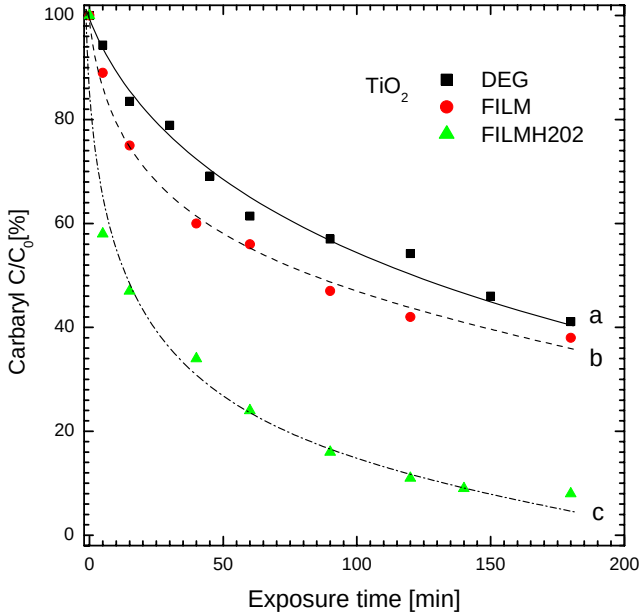

Fig. 4. Photocatalytic degradation curves of carbaryl under concentrated solar irradiation and using (a) Degussa P-25 and (b) TiO_2 thin films as catalysts. Curve (c) is the same as (b) but adding H_2O_2 as oxidant agent.

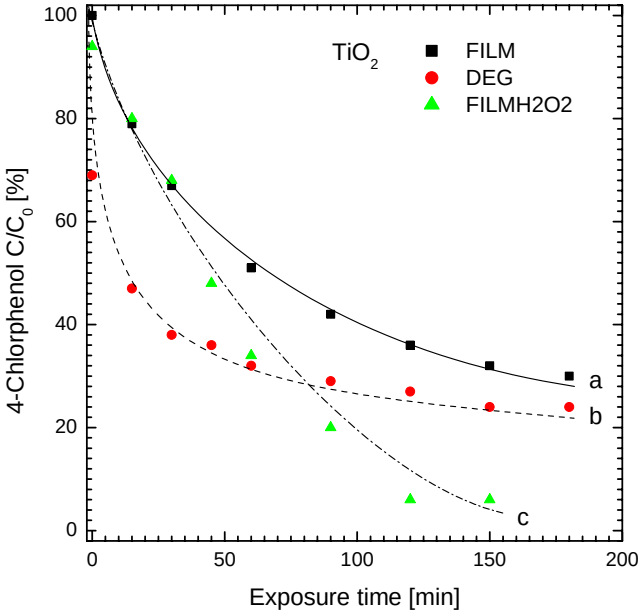

Fig. 5. Photocatalytic degradation curves of 4-chlorophenol under concentrated solar irradiation and using (a) Degussa P-25 and (b) TiO_2 thin films as catalysts. Curve (c) is the same as (b) but adding H_2O_2 as oxidant agent.

process but only to show the applicability of the fixed catalyst so, for comparison, the final carbaryl concentration in the fixed and powder forms has been considered.

For TiO_2 films catalyst, final concentrations of carbaryl after 140 min of irradiation were equivalent to 34% of the initial concentration when measuring the UV adsorption. According to these results, both forms of the catalyst give similar results. As a matter of fact the estimated final carbaryl concentration is lower when using TiO_2 films.

3.5. Degradation of 4-chlorophenol

Fig. 5 shows photocatalytic degradation curves describing the diminishing of the 4-chlorophenol concentration as a function of exposure time to the solar irradiation and using (a) Degussa P-25 and (b) TiO_2 thin films as catalysts. Curve (c) is the same as (b) but adding H_2O_2 as the oxidant agent. The first difference between the powder and the fixed form of catalyst is the great adsorption capability of the powder towards 4-chlorophenol. As soon as the powder is in contact with the spiked water, 4-phenol is quickly adsorbed by the catalyst, which is not observed in the immobilized form. Although for both systems the initial concentration is the same, the less than 5 min, needed to form a homogenous suspension with the powder, are enough to cause around 30% of adsorption of the organic pollutant. This effect explains the difference at the point zero for the curves.

After 3 h of concentrated solar irradiation, the final dissolved concentration of 4-chlorophenol is 24% of its initial value for the Degussa P-25 and 29% for the TiO_2 immobilized catalysts, respectively. This means that both forms of the catalyst have approximately the same photoefficiency. Since the use of the fixed catalyst avoids many operational complications for separation of the powder catalyst, this represents a great advantage towards the application of this technology.

3.6. Photocatalysis + hydrogen peroxide

As it is well known, the use of hydrogen peroxide has been an alternative to improve the photooxidation of organic pollutants catalyzed by TiO_2. In the present job, absorbance measurements were used to estimate the degraded concentration of carbaryl and 4-chlorophenol using TiO_2 thin films as catalyst and H_2O_2 as oxidant agent. The enhancing effect is well appreciated in Figs. 4 and 5 where the aqueous concentration of carbaryl and 4-chlorophenol was reduced, respectively, almost at 10% of its initial value. However, during the experiments a bit of the film was peeled off. In additional tests it was demonstrated that TiO_2 films over glass plane substrates did not suffer the peeling observed for the cylindrical geometry, so it has been associated with the loss of material that was not well adhered. In any case, the use of hydrogen peroxide must be carefully considered, as it must be neutralized before analysis of target compound, and it is highly recommended to treat the excess before final disposal of treated water.

3.7. Reduction of the toxicity

The toxicity determination for the initial and after treatment water samples generates the values shown in Table 1. It

Table 1
Values of EC_{50} for initial and final samples in 4-chlorophenol photocatalysis

Sample	EC_{50}
Initial 4-chlorophenol	5
4-Chlorophenol after treatment (fixed TiO_2)	15
4-Chlorophenol after treatment (Degussa)	6

is important to note that a sample with a high value of EC_{50} has to be diluted more times than another one with a smaller EC_{50} value, to cause the same effect on the test organism, so the higher the EC_{50} the lower toxicity of the sample.

It should be noted that when using TiO_2 powder, the toxicity remains high but it is reduced in an important manner when the fixed form of TiO_2 is used as photocatalyst. In order to clarify the detailed mechanisms governing photodegradation for the fixed catalyst, it is necessary to conduct additional experiments. A possible explanation for the differences is related to the complex phenomena of adsorption–desorption of the test pollutant as well as those of the photooxidation products that modifies the distribution and abundance of species [11] hence leading to different values of measurable toxicity.

4. Conclusions

TiO_2 films were effective for detoxification of water polluted with carbaryl and 4-chlorophenol. Final degradation results using the immobilized TiO_2 catalyst are comparable to those obtained with Degussa P-25 powder, which is recognized as one of the most efficient forms of titanium dioxide in photocatalysis. The use of fixed catalysts has very important operational advantages. On the one hand, it does not require separation steps before analysis or at the end of the photocatalytic treatment. Accordingly, there is no generation of residual catalyst. Additionally, it can be self-cleaned after use just passing water and exposing the wet glass matrix to the sun. On the other hand, the immobilized catalyst allows us to carry out measurements on TiO_2, like electrical conductivity and photosensitivity, which are very difficult to make in powder.

The presented material is an easy-to-prepare material that offers great operational advantages. Our current job looks for higher photoefficiencies as well as determination of its operating life in continuous highly demanding daily process. In addition, complementary studies to get a thorough knowledge of the oxidation of organic pollutants with immobilized TiO_2 are under way.

Acknowledgements

This work was partially supported by CONACYT (México) through research grants 37636-U and G 38618-U, and by DGAPA (Project Nr. IN109200). The authors want to thank valuable comments from Claudio Estrada, Ma. Teresa Leal and Erick Bandala as well as the technical assistance from R. Morán Elvira.

References

[1] A. Fujishima, T.N. Rao, D.A. Tryk, J. Photochem. Photobiol. C: Photochem. Rev. 1 (2000) 1–21.
[2] S. Malato, J. Blanco, C. Richter, M.I. Maldonado, Appl. Catal. B: Environ. 25 (2000) 31–38.
[3] S. Malato, J. Blanco, A. Vidal, C. Richter, Appl. Catal. B: Environ. 37 (2002) 1–15.
[4] R. Pozzo, M. Baltanás, A. Cassano, Catal. Today 54 (1999) 143–157.
[5] N. Negishi, T. Iyoda, K. Hashimoto, A. Fujishima, Chem. Lett. (1995) 841–842.
[6] A. Rachel, M. Subrahmanyam, P. Boule, Appl. Catal. B: Environ. 37 (2002) 301–308.
[7] Ch. Guillard, B. Beaugiraud, C. Dutriez, J.M. Herrmann, H. Jaffrezic, N. Jaffrezic-Renault, M. Lacroix, Appl. Catal. B: Environ. 39 (2002) 331–342.
[8] H. Al-Ekabi, N. Serpone, J. Phys. Chem. 92 (1988) 5726–5731.
[9] H. Al-Ekabi, N. Serpone, E. Pelizzetti, C. Minero, M.A. Fox, B. Draper, Langmuir 5 (1989) 250–255.
[10] J.M. Tseng, C.P. Huang, Wat. Sci. Tech. (Kyoto) 23 (1991) 377–387.
[11] U. Stafford, K.A. Gray, P. Kamat, J. Catal. 167 (1997) 25–32.
[12] M. Gu Kan, H.-E. Han, K.-J. Kim, J. Photochem. Photobiol. A: Chem. 125 (1999) 119–125.
[13] T. Yoko, K. Kamiya, S. Sakka, Yogyo-Kyokai-Shi 95 (2) (1987) 150–155.
[14] A. Jiménez, C. Estrada, A.D. Cota, A. Román, Solar Energy Mater. Solar Cells 60 (2000) 85–95.
[15] A.D. Eaton, L.S. Clesceri, A.E. Greenberg (Eds.), Standard Methods for the Examination of Water and Wastewater, 19th ed., APHA, AWWA, WEF, 1995.
[16] B.D. Cullity, Elements of X-ray Diffraction, Addison-Wesley, Menlo Park, 1978.
[17] A.M. Bokhimi, O. Novaro, T. López, E. Sánchez, R. Gómez, J. Mater. Res. 10 (11) (1995) 2788–2796.
[18] O. Madelung, Introduction to Solid State Theory, Springer Series in Solid State Sciences 2, Springer-Verlag, Berlin, 1981.
[19] R.A. Smith, Semiconductors, Cambridge University Press, London, 1978.
[20] M. Radecka, K.Z. Akrzewska, H. Czternastek, T. Stapinski, S. Debrus, Appl. Surf. Sci. 65–66 (1993) 227.
[21] P. Kopfstadt, Nonstoichiometry, Diffusion and Electrical Conductivity in Binary Metal Oxides, Krieger, Malabar, FL, 1983.
[22] F.H. Kroeger, H. Vink, in: F. Seitz, D. Turnbull (Eds.), Solid State Physics, vol. 3, Academic Press, New York, 1956.
[23] O. Brahmia, C. Richard, Photochem. Photobiol. A: Chem. 156 (2003) 9–14.